RESEARCH ARTICLE

Human Mutation

OFFICIAL JOURNAL HGVS HUMAN GENOME VARIATION SOCIETY www.hgvs.org

# Antisense Therapeutics for Neurofibromatosis Type 1 Caused by Deep Intronic Mutations

Eva Pros,[1,2] Juana Fernández-Rodríguez,[1] Belén Canet,[1] Llúcia Benito,[3] Aurora Sánchez,[4] Ana Benavides,[5] Feliciano J. Ramos,[6] María Asunción López-Ariztegui,[7] Gabriel Capellá,[1] Ignacio Blanco,[3] Eduard Serra,[2] and Conxi Lázaro[1]*

[1]*Laboratori de Recerca Translacional, Institut Català d'Oncologia–Institut d'Investigació Biomèdica de Bellvitge (IDIBELL), L'Hospitalet de Llobregat, Barcelona, Spain*

[2]*Departament de Genètica, Institut d'Investigació Biomèdica de Bellvitge (IDIBELL), L'Hospitalet de Llobregat, Barcelona, Spain*

[3]*Unitat de Consell Genètic, Institut Català d'Oncologia, L'Hospitalet de Llobregat, Barcelona, Spain*

[4]*Secció de Citogenètica i Genètica Clínica, Servei de Bioquímica i Genètica, Barcelona, Spain*

[5]*Servicio de Genética, Hospital Universitario Central de Asturias (HUCA), Oviedo, Spain*

[6]*Departamento de Pediatría, Facultad de Medicina, Universidad de Zaragoza, Zaragoza, Spain*

[7]*Servicio de Genética, Hospital de Cruces, Bilbao, Vizcaya, Spain*

Communicated by David N. Cooper

Received 28 July 2008; accepted revised manuscript 7 October 2008.
Published online 20 February 2009 in Wiley InterScience (www.interscience.wiley.com). DOI 10.1002/humu.20933

**ABSTRACT:** Neurofibromatosis type 1 (NF1) is an autosomal dominant disorder affecting 1:3,500 individuals. Disease expression is highly variable and complications are diverse. However, currently there is no specific treatment for the disease. NF1 is caused by mutations in the *NF1* gene, approximately 2.1% of constitutional mutations identified in our population are deep intronic mutations producing the insertion of a cryptic exon into the mature mRNA. We used antisense morpholino oligomers (AMOs) to restore normal splicing in primary fibroblast and lymphocyte cell lines derived from six NF1 patients bearing three deep intronic mutations in the *NF1* gene (c.288+2025T>G, c.5749+332A>G, and c.7908-321C>G). AMOs were designed to target the newly created 5′ splice sites to prevent the incorporation of cryptic exons. Our results demonstrate that AMO treatment effectively restored normal *NF1* splicing at the mRNA level for the three mutations studied in the different cell lines analyzed. We also found that AMOs had a rapid effect that lasted for several days, acting in a sequence-specific manner and interfering with the splicing mechanism. Finally, to test whether the correction of aberrant *NF1* splicing also restored neurofibromin function to wild-type levels, we measured the amount of Ras-GTP after AMO treatment in primary fibroblasts. The results clearly show an AMO-dependent decrease in Ras-GTP levels, which is consistent with the restoration of neurofibromin function. To our knowledge this is the first time that an antisense technique has been used successfully to correct *NF1* mutations opening the possibility of a therapeutic strategy for this type of mutation not only for NF1 but for other genetic disorders.
Hum Mutat 30, 454–462, 2009.


**KEY WORDS:** neurofibromatosis 1; NF1; morpholino; antisense oligonucleotide therapy; AMO; deep intronic mutation

## Introduction

Neurofibromatosis type 1 (NF1; MIM# 162200) is a common autosomal dominant disorder characterized mainly by the presence of café-au-lait spots (CLS), cutaneous neurofibromas, Lisch nodules, inguinal and axillary freckling [Riccardi, 1992], and a high predisposition to develop certain types of tumors. It is caused by mutations in the *NF1* gene, which spans approximately 300 kb of genomic DNA, contains 57 constitutive exons and encodes for an 11–13-kb mRNA transcript [Li et al., 1995; reviewed in Viskochil, 1998]. The *NF1* gene product, neurofibromin, includes 2,818 amino acids, is widely expressed in most tissues and contains a well-defined domain, the GAP-related domain (GRD). The main known function of neurofibromin is the negative regulation of Ras by enhancing its intrinsic GTPase activity [Xu et al., 1990]. *NF1* acts as a tumor suppressor gene, thus somatic mutations have been found in several NF1-associated tumors (discrete and plexiform neurofibromas, malignant peripheral nerve sheath tumors, gastrointestinal tumors, astrocytomas, and juvenile myelomonocytic leukemia) and in other traits (CLS and tibial pseudoarthrosis) [De Raedt et al., 2008].

An important part of point mutations in the *NF1* gene affects the correct mRNA splicing, representing about 30% in the largest unbiased comprehensive study of >2,000 unrelated *NF1* patients (Ludwine Messiaen, personal communication) and 44% of our identified mutations, screened by a cDNA single-strand conformation polymorphism and heteroduplex (cDNA-SSCP/HD)

Eva Pros and Juana Fernández-Rodríguez contributed equally to this work.

*Correspondence to: Conxi Lázaro, Ph.D., Laboratori de Recerca Translacional, Institut Català d'Oncologia, Hospital Duran i Reynals, Gran Via s/n, km 2.7, L'Hospitalet de Llobregat, 08907, Spain. E-mail: clazaro@iconcologia.net

Contract grant sponsors: Carlos III Health Institute (BF03/00455, ISCIIIPI05/1149, and ISCIIIRETICRD06/0020/1051); Spanish Ministry of Education and Science (SAF2005-00833 and SAF2006-05399) and Catalan Health Institute and Autonomous Government of Catalonia (2005SGR00018).

mutational screening approach [Ars et al., 2000; Pros et al., 2008]. Most splice mutations disrupt canonical splice sequences (5′ donor site, 3′ acceptor site, or the branch point) while others create novel splice sites or affect splicing regulatory elements. The effect of these mutations on mRNA is dependent on the sequence context and could result in the following: exon skipping, deletion of part of an exon, or intron inclusion [Wimmer et al., 2007; Pros et al., 2008]. A small subset of these mutations are single-nucleotide changes in sequences deep inside introns creating either a novel donor or acceptor site that, in conjunction with a nearby cryptic splice counterpart, defines a new cryptic exon that spliceosome includes into mature messenger. In our population these mutations represent approximately 2.1% of the total number of identified germline mutations [Messiaen and Wimmer, 2008; Pros et al., 2008]. A high percentage of these mutations create a premature termination codon (PTC) that is susceptible to degradation by the nonsense-mediated mRNA decay (NMD) mechanism.

Deep intronic mutations are good targets for therapeutic correction because they are not located in the coding region and they leave wild-type splice sites intact. The inactivation of a newly created splice site by antisense oligonucleotides (AONs) prevents the splicing machinery from recognizing the cryptic exon and promotes normal splicing. AONs have been used to correct splicing or to restore the reading frame in several genetic disorders, including β-thalassemia [Sierakowska et al., 1996], cystic fibrosis [Friedman et al., 1999], and Duchenne muscular dystrophy [van Deutekom et al., 2001].

Among AONs, antisense phosphorodiamidate morpholino oligomers (AMOs) are analogs of oligonucleotides with a six-membered morpholino ring replacing ribose or deoxyribose. AMOs have high binding specificity, stability, and resistance to nucleases, and their activity is highly durable [Summerton and Weller, 1997]. Due to these advantageous properties, AMOs are used for therapeutical purposes for several disorders including β-thalassemia [Lacerra et al., 2000; Suwanmanee et al., 2002a], Duchenne muscular dystrophy [McClorey et al., 2006], Hutchinson-Gilford progeria syndrome [Scaffidi and Misteli, 2005], ataxia telangiectasia [Du et al., 2007], and propionic and methylmalonic acidemias [Rincon et al., 2007].

In this study we designed specific AMOs to block the effect of three independent *NF1* deep intronic mutations causing the inclusion of cryptic exons in six NF1 patients. We derived cell lines from these patients and treated them with the designed AMOs. We evaluated the effect of the AMOs on *NF1*-mRNA splicing and their specificity, stability, and mode of action. In addition, we indirectly assessed neurofibromin function after AMO treatment by measuring active Ras (bound to GTP). The results show that AMO treatment could be an effective approach for correcting *NF1* expression deficiency in patients with deep intronic mutations.

## Materials and Methods

### Patients and Mutations

Six patients carrying three deep intronic mutations in the *NF1* gene were recruited for this study (Table 1). All patients were previously informed about the aims of the research and gave the necessary consent with institutional review board (IRB) approval. Skin biopsy and peripheral blood were acquired from all patients to isolate and culture primary fibroblasts and lymphocyte cells, respectively.

All patients fulfill the established NF clinical diagnostic criteria. All present CLS, freckling, Lisch nodules, and neurofibromas. One of the patients (Patient 3) has a NF1-Noonan phenotype; three patients (Patients 2, 4, and 5) have classical NF1 phenotype without any remarkable feature, and the two remaining patients (Patients 1 and 6) are characterized by a small number of neurofibromas according to their age.

The nomenclature for mutations at the DNA level, their effect at the mRNA level, and the predicted protein was determined according to the guidelines of the Human Genome Variation Society (www.hgvs.org). The first nucleotide of the first methionine codon is denoted position +1 according to the *NF1* mRNA sequence RefSeq NM_000267.2.

### Splice-Site Strength Prediction

The strength of the pseudoexon splice sites was analyzed using the following methods: 1) a neural network approach, which uses a machine-learning technique that is trained to recognize sequence patterns on the basis of a set of DNA sequences encompassing authentic splice sites [Reese et al., 1997] (a default level of 0.01 was used for all calculations; www.fruitfly.org/seq_tools/splice.html); 2) a first-order Markov model, which takes into account only dependencies between adjacent positions within the splice-site sequence, and a maximum entropy model, which takes into account dependencies between adjacent and nonadjacent positions [Burge, 1998; Yeo and Burge, 2004] (http://genes.mit.edu/burgelab/maxent/Xmaxentscan_scoreseq.html); and 3) the Shapiro and Senapathy position-weight matrix, which reflects the degree of conservation at each position of the consensus 5′ and 3′ splice motifs (http://ast.bioinfo.tau.ac.il/SpliceSiteFrame.html) [Senapathy et al., 1990; Shapiro and Senapathy, 1987]. For each method, a high score indicates a greater probability of the corresponding sequence being used as a splice site, although it does not represent an absolute predictive value. Upper limits are defined only for the Shapiro and Senapathy (upper limit: 100) and neural network (upper limit: 1) predictive methods.

### Cell Lines and Cultures

For fibroblast isolation, skin was cut into small pieces and digested with 160 U/ml collagenase type 1 (Sigma, St. Louis, MO) and 0.8 U/ml dispase grade 1 (Roche Diagnostics, Penzberg,

**Table 1. Details of *NF1* Deep Intronic Mutations Studied***

| DNA mutation | Patient | Intron | mRNA effect | Putative protein | AMO |
|---|---|---|---|---|---|
| c.288+2025T>G | 1 | 3 | r.288_289ins288+1917_288+2024 | p.Gln97X | IVS3-AMO |
| c.5749+332A>G | 2, 3 | 30 | r.5749_5750ins5749+155_5749+331 | p.Ser1917ArgfsX12 | IVS30-AMO |
| c.7908-321C>G | 4[a], 5[a], 6 | 45 | r.7907_7908ins7908-322_7908-391 | p.His2637SerfsX2 | IVS45-AMO |

*Sequence changes are described at the cDNA level (indicated by "c."). The +1 nucleotide corresponds to the A of the ATG translation initiation codon in the reference sequence NM_000267.2.

[a]Patients from the same family.

Germany [Serra et al., 2001]. Fibroblasts were grown with Dulbecco's modified Eagle's medium (DMEM; Gibco, Invitrogen, Paisley, UK), 10% fetal bovine serum (FBS; Gibco, Invitrogen), and penicillin/streptomycin (Gibco, Invitrogen) at 37°C and 5% $CO_2$.

Lymphocyte cell cultures were established by Epstein-Barr virus (EBV) transformation and maintained in RPMI medium 1640 (Gibco, Invitrogen) with 10% inactivated FBS (Gibco, Invitrogen) and penicillin/streptomycin (Gibco, Invitrogen) at 37°C and 5% $CO_2$.

## Morpholino Oligomer Design and Treatment

The 25-mer AMOs were designed, synthesized, and purified by Gene Tools (Philomath, OR) and targeted the newly created aberrant splice site for the three studied *NF1* mutations. Endo-Porter (GeneTools) was used to deliver AMOs into cells. AMO sequences were as follows: 5′-CTTTCACTTA**C**ATATTCCAAC-TATG-3′ (IVS3-AMO, mutation c.288+2025T>G); 5′-ACATG-GATACTTA**C**GTGGACTTTTC-3′ (IVS30-AMO, mutation c.5749 +332A>G); and 5′-CTGTCTGCTACTTA**C**CATGTTTTAG-3′ (IVS45-AMO, mutation c.7908-321C>G) (mutation sites are in bold) (Fig. 1).

For fibroblast cell line treatment with AMO, cells were seeded at $3 \times 10^5$ cells/well, in a 6-well plate. The next day, culture medium was replaced by fresh 10% FBS/DMEM medium containing the indicated concentrations of AMO (see Results). Immediately after, Endo-Porter was added and mixed well (6 μM).

For lymphocyte treatment with AMO, $8 \times 10^5$ cells were resuspended in RPMI 1640 medium without FBS and seeded in a 12-well plate (1 ml/well). AMO was added directly to the medium at the indicated concentrations (see Results). Endo-Porter was added to the medium and mixed properly (10 μM). After 4 hr, FBS was added, to a final concentration of 5%.

In each experiment, untreated cells with the same concentration of Endo-Porter were used as controls. Each experiment was performed in triplicate.

## RNA Preparation, RT-PCR, and Quantification of *NF1* Expression

Total RNA was extracted by using the RNeasy Mini Kit (Qiagen, Heidelberg, Germany) following the manufacturer's instructions. Reverse-transcription reactions were performed using 1–2 μg of total RNA with random hexamers and SuperScript II Reverse Transcriptase (Invitrogen). PCR reactions were performed under the following conditions: 30 cycles of 94°C for 30 sec, 60°C for 30 sec, and 72°C for 1 min after an initial denaturation of 3 min, and followed by a final extension of 8 min. The primer sequences used to amplify both wild-type transcripts and the different transcripts with cryptic exon inclusion are available upon request. PCR products were analyzed with the Agilent 2100 bioanalyzer with DNA 1000 LabChip kit series II (Agilent Technologies, Waldbronn, Germany). Percentages of cryptic exon inclusion were obtained by taking the sum of concentration values (nmol/l) of the different fragments (wild-type and aberrantly spliced) as 100%.

## Assessing the Specificity and Mode of Action of AMO

### *NMD analysis*

To verify that NMD was not interfering in the restorative effect observed after AMO treatment, fibroblast cell lines were treated with 200 μg/ml puromycin (an inhibitor of NMD) (Sigma) 4–6 hr before RNA extraction [Andreutti-Zaugg et al., 1997] in both cell cultures treated with or without AMOs.

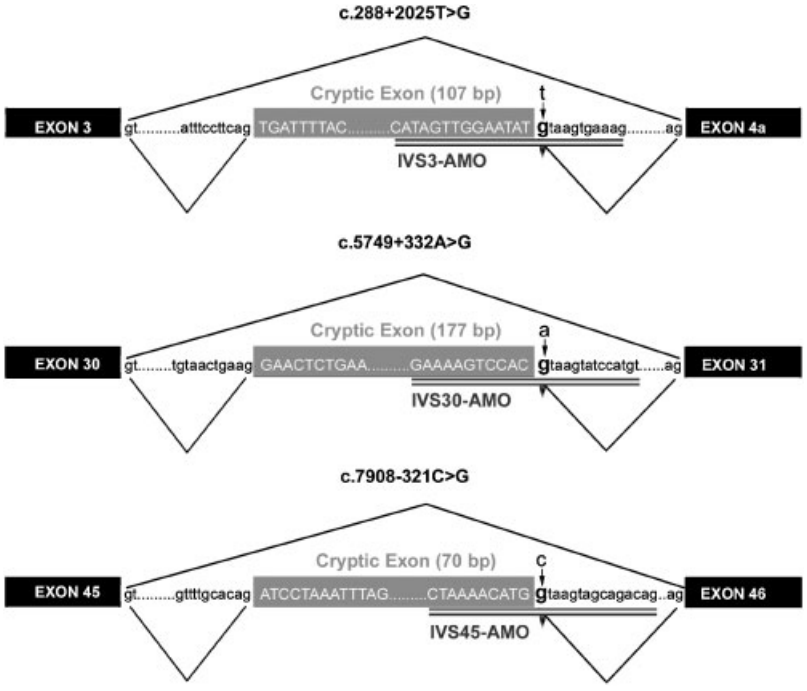


**Figure 1.** Schematic representation of three *NF1* deep intronic mutations and specific AMO location. Constitutive and cryptic exons are represented by dark and light gray boxes, respectively. The boundaries of cryptic inserted exons are shown by uppercase sequences; flanking intronic sequences are shown in lowercase. AMO sequences are underlined and the specific names are written below. Mutated nucleotides are shown in bold and nucleotide changes are indicated by an arrow.

### *Wild-type NF1 transcript normalization with cyclophilin gene expression*

To quantify the expression of the *NF1* gene relative to that of a control gene, RT-PCR analysis was performed using primers to amplify *NF1* and a cyclophilin gene in the same multiplex reaction [Pluvinet et al., 2004]. No change in cyclophilin gene expression was observed in the experimental conditions used, so this gene was chosen as a reference for normalizing the quantification of *NF1* transcripts generated.

### *Assessing the expression of both NF1 alleles*

The expression of the two *NF1* alleles was assessed by analyzing a heterozygous exonic polymorphism by cDNA-SSCP analysis as described previously [Serra et al., 2000] and by sequence analysis of the region containing the polymorphism. First, all six patients were genotyped for the most common exonic polymorphisms described in the *NF1* gene to identify heterozygous patients. Only Patient 3 was found to be heterozygous for the SNP polymorphism in exon 13 (c.2034A>G) [Regnier et al., 1995]. Primers and PCR conditions are available upon request.

## Ras-GTP Assay and Western Blot of Total Ras

The Ras activation assay kit (Upstate Millipore, Temecula, CA) was used according to the manufacturer's protocol. The assay uses affinity precipitation to isolate Ras-GTP from cell lysate. Fibroblast cell lysate (300 μg) was incubated with an agarose-bound Raf-1 RBD fusion protein. Agarose beads were collected by pulsing in a microcentrifuge (10 sec at 14,000 *g*), washed with lysis buffer, and resuspended in Laemmli sample buffer.

Cell lysates containing 5 μg of protein were prepared for Western blot analysis of total Ras.

The samples from the Ras-GTP assay and total Ras analysis were then boiled for 5 min and loaded onto 12% SDS-PAGE polyacrylamide gels. Samples were electrophoresed and transferred (400 mA) to a nitrocellulose membrane (Amersham Hybond-C extra; GE-Healthcare, Little Chalfont, UK). The membrane was blocked with 5% nonfat dry milk and incubated overnight at 4°C with primary antibody, anti-Ras clone RAS10 (1/300; Upstate, Millipore) (1 μg/ml). This was followed by incubation with horseradish peroxidase (HRP)-conjugated secondary antibody at room temperature for 1 hr. The blot was developed using the West Pico SuperSignal substrate (Pierce Technology, Rockford, IL) for the total Ras analysis and Tubulin and West Femto SuperSignal (Pierce Biotechnology) for the Ras-GTP assay.

# Results

## Nature of Mutations and Design of Specific Morpholino Oligomers

In our routine clinical setting, 2.1% of identified mutations are deep intronic nucleotide changes causing the inclusion of cryptic exons [Pros et al., 2008]. To test the efficiency of AMO treatment in restoring normal splicing for this mutation type, we contacted all available patients and invited them to participate in the study. Six patients were recruited and primary fibroblasts and EBV-transformed lymphocyte (or lymphoblastoid) cell lines were established for each patient. The patients harbored three different mutations (Fig. 1; Table 1), all of which created new cryptic 5′ splice sites. According to the splice-site predictors used, the three nucleotide changes gave excellent scores for donor site (Table 2), whereas the wild-type sequences gave different scores. The 3′ acceptor site used to insert the cryptic exon gave good scores for 2 out of the 3 mutations studied. However, the 3′ splice-sites (ss) for mutation in intron 30 gave a score of zero in the neural network program and low values in the maximum entropy model and the first-order Markov model (the score for the Shapiro and Senapathy position-weight matrix was intermediate) (Table 2). These results suggest that other factors different to the strength of the splice sites define this cryptic exon [Wimmer et al., 2007].

Three AMOs were designed to block the recognition of the newly created 5′ splice sites, thus forcing normal splicing and preventing the inclusion of the cryptic exon (Fig. 1).

## Correction of *NF1* Aberrant Splicing by AMOs in Different Cell Types

We first set up AMO treatment conditions using fibroblasts from a single patient per mutation. After establishing the optimal conditions we used fibroblasts and EBV-transformed lymphocytes from all mutations. To determine the effect of AMO concentration on aberrant splicing correction, a dose-response experiment was conducted by treating fibroblasts with three different AMO concentrations (5 μM, 10 μM, and 20 μM) for 24 hr (Fig. 2A). For the three mutations studied we observed that the percentage of aberrantly-spliced transcripts (containing the cryptic exon) was approximately 10 to 15% of the total *NF1* mRNA (wild-type+aberrantly-spliced transcripts) without AMO treatment (Fig. 2A). The low percentage of cryptic exon-containing *NF1* mRNAs was due to their partial degradation by the NMD machinery, since cryptic exon inclusion created a premature stop codon in all cases (see the section Assessing the Mode of Action of AMO, below).

**Table 2. 5′ and 3′ Splice Sites and Predicted Scores***

| | 5′ splice-site (donor) sequence and scores | | | | | 3′ splice-site (acceptor) sequence and scores | | | | |
|---|---|---|---|---|---|---|---|---|---|---|
| DNA mutation | Sequence | S&S | NN | ME | MM | Sequence | S&S | NN | ME | MM |
| c.288+2025T>G | TAT TTAAGT wt; | 66.31; | 0; | –1.81; | –3.27; | AATTGTTTTATTTCCTTCAG TGA | 90.06 | 0.67 | 7.65 | 8.99 |
| | TAT **G**TAAGT mut | 83.43 | 0.98 | 6.69 | 5.24 | | | | | |
| c.5749+332A>G | CAC ATAAGT wt; | 69.65; | 0; | 1.97; | 1.54; | GTGGTATCCTGTAACTGAAG GAA | 75.38 | 0 | 1.24 | 3.11 |
| | CAC **G**TAAGT mut | 86.77 | 1.00 | 10.16 | 9.72 | | | | | |
| c.7908-321C>G | ATG CTAAGT wt; | 74.10; | 0; | 2.74; | 1.83; | TTTCTTTTTGTTTTGCACAG ATC | 90.36 | 0.95 | 10.34 | 11.43 |
| | ATG **G**TAAGT mut | 91.22 | 0.99 | 11.01 | 10.10 | | | | | |

*Nucleotides introduced by mutations are in bold. Splice-site strength scores (described in the Materials and Methods section) are obtained using the Shapiro and Senapathy (S&S) consensus splice-site weight matrix, neural network (NN) prediction, first-order Markov models (MM), and a maximum entropy (ME) model. A higher score indicates a greater probability of the resulting sequence being used as a splice site.

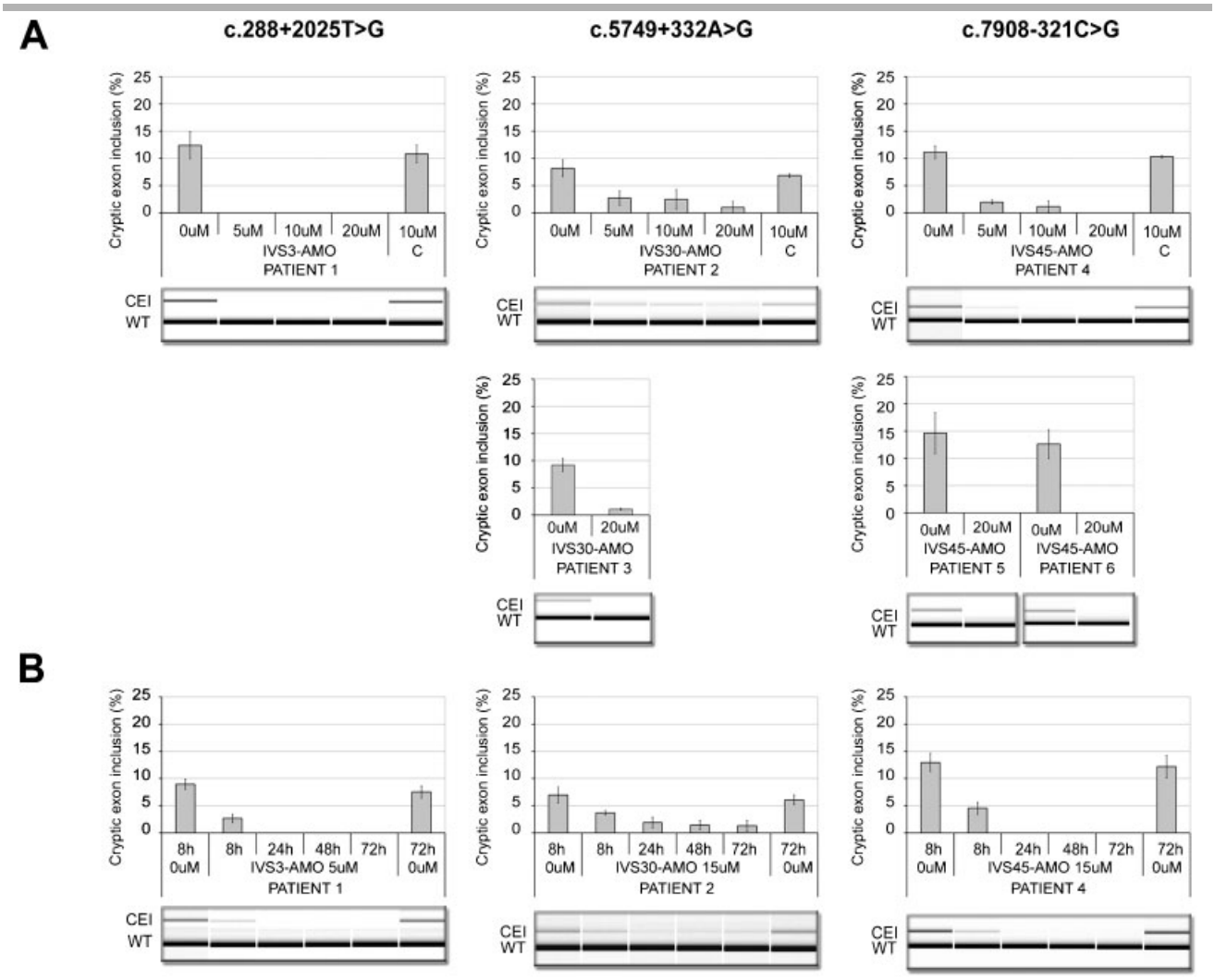


**Figure 2.** Correction of aberrant splicing by AMO treatment of fibroblast cultures bearing the three studied mutations: c.288+2025T>G, c.5749+332A>G, and c.7908–321C>G. RT-PCR analysis of total RNA was performed using specific primers to analyze both transcripts (wild-type and cryptic exon–containing transcripts). The y-axes of each graph show the proportion of cryptic exon–containing transcripts vs. the total. The data are represented by a bar consisting of the mean ± SD for at least three independent experiments. The corresponding Agilent electrophoresis gel is shown below each graph. **A:** Upper part: dose response after 24 hr of treatment using different AMO concentrations (5, 10, and 20 μM). Controls for AMO specificity (C) were: IVS30-AMO, IVS45-AMO, and IVS3-AMO for c.288+2025T>G, c.5749+332A>G, and c.7908–321C>G mutations, respectively. Lower part: AMO correction was also observed in three additional patients with mutations c.5749+332A>G (Patient 3) and c.7908–321C>G (Patients 5 and 6) (using 20 μM). **B:** Time course with the indicated AMO treatment. CEI: cryptic exon inclusion; WT: wild-type.

After cells were treated with the specifically designed AMO, complete correction of aberrant splicing was observed at 5 μM concentration in Patient 1 (c.288+2025T>G). In Patients 2 (c.5749+332A>G) and 4 (c.7908-321C>G) a dose-dependent correction of aberrant splicing was observed, which was found to be complete at 20 μM in Patient 4 (c.7908–321C>G) and almost complete in Patient 2 (c.5749+332A>G). More patients were available for the mutations c.5749+332A>G (Patient 3) and c.7908–321C>G (Patients 5 and 6) (Table 1), and these patients were analyzed under the optimal AMO treatment conditions. All patients bearing the same constitutional mutation exhibited similar results (Fig. 2A).

The specificity of the different AMOs in each case was assessed by using a different control AMO that had been designed to correct the effect of one of the other two studied mutations (C in Fig. 2A). Only mutation-specific AMO had a corrective effect on aberrant splicing in all cases, which indicated that the effect of AMO treatment was sequence-specific.

To evaluate the effect of time on mutation correction after morpholino treatment, a time course was performed for the three mutations in fibroblast cell lines (Fig. 2B). The morpholino concentration used was the same or lower than the concentration at which complete (or almost complete) correction was observed at 24 hr (i.e., 5 μM in cells derived from Patient 1 and 15 μM in cells derived from Patients 2 and 4, respectively). Transcriptional analysis was performed at different time points ranging from 8 to 72 hr (Fig. 2B). A considerable correction of aberrant splicing was observed as early as 8 hr after AMO treatment. For example, in Patient 1 (c.288+2025T>G) the proportion of aberrant transcripts after 8 hr of treatment was reduced from 9% ± 0.9 to 2.7% ± 0.8. Complete decrease of aberrant transcripts was observed at 24 hr in Patients 1 and 4 and lasted for at least 72 hr. Reversion of aberrant splicing, although not complete, was observed for the mutation located in intron 30, with the maximum decrease of aberrant transcripts found between

48–72 hr following treatment with 15 μM AMO (Fig. 2B). In general, the efficiency of *NF1* splicing correction in fibroblasts after 24 hr of treatment ranged from 87 to 100% in the different mutations.

We then compared the effects of AMO treatment in a different cell type by testing aberrant splicing correction in transformed lymphocytes from the same patients. The maximum correction (not complete) was observed at 72 hr following treatment with 50 μM AMO in Patient 1 (c.288+2025T>G) (Fig. 3A). Lower concentrations were also tested but these were not as effective (data not shown). We used the same conditions to analyze lymphocyte cell lines for the other mutations (c.5749+332A>G and c.7908–321C>G) and patients. We observed higher transcriptional restoration in Patients 1 and 4 (bearing c.288+2025T>G and c.7908–321C>G mutations, respectively) (Fig. 3B) than in Patients 2 and 3 (bearing the c.5749+332A>G mutation). In general, a lower degree of aberrant splicing correction (30–70%) was observed in transformed lymphocyte cell lines, and a higher concentration of morpholino together with a longer time of exposure was needed to produce similar effects to those seen in fibroblasts. We believe that these differences are due to the greater difficulty of lymphocyte transfection (see Discussion).

Finally, to test the stability and duration of the effect of AMO treatment in correcting aberrant splicing, two fibroblast primary cell cultures were treated with AMO and cells were harvested at different time points over 20 days (Fig. 4). For mutation c.288+2025T>G (Patient 1), no transcripts containing cryptic exons were observed, even at day 20. In contrast, for mutation c.5749+332A>G (Patient 2), trace levels of aberrantly-spliced mRNAs were observed at day 13 at 30 μM of AMO, although in a lower proportion than in untreated cells (Fig. 4). However, in silver-stained polyacrylamide gels, which are more sensitive than ethidium bromide–stained gels, traces of aberrantly-spliced mRNAs were observed at days 10 and 3, for mutations in c.288+2025T>G and c.5749+332A>G, respectively (data not shown).

## Assessing the Mode of Action of AMO

The three deep intronic mutations considered in this study lead to the inclusion of a cryptic exon that, in turn, produces mRNA transcripts with a frameshift in the open reading frame. This change generates transcripts with a PTC that are susceptible to degradation by the NMD pathway. To rule out the possibility that the observed decrease of aberrant transcripts after AMO treatment was due to an enhancement of the NMD pathway, we treated fibroblasts from different patients with puromycin (a NMD inhibitor) in the presence or absence of AMO (Fig. 5A). For the three studied mutations we observed an increase in transcripts containing the cryptic exon after puromycin treatment (in the absence of AMO), which confirmed that a certain proportion of aberrantly transcribed mRNAs was degraded by the NMD machinery. However, there was also a total or considerable correction of aberrant splicing after AMO treatment (depending on the mutation, see Fig. 5A) in the presence of puromycin, which indicates that the AMOs acted directly on *NF1* splicing, independently of the NMD mechanism.

The analysis of aberrantly-spliced *NF1* mRNAs was quantified by calculating the relative proportion of cryptic exon inclusion transcripts vs. wild-type transcripts. We also decided to determine whether the correction of aberrant splicing (i.e., a decrease in the amount of cryptic exon–containing mRNAs) correlated with an increase in the levels of wild-type transcripts after AMO

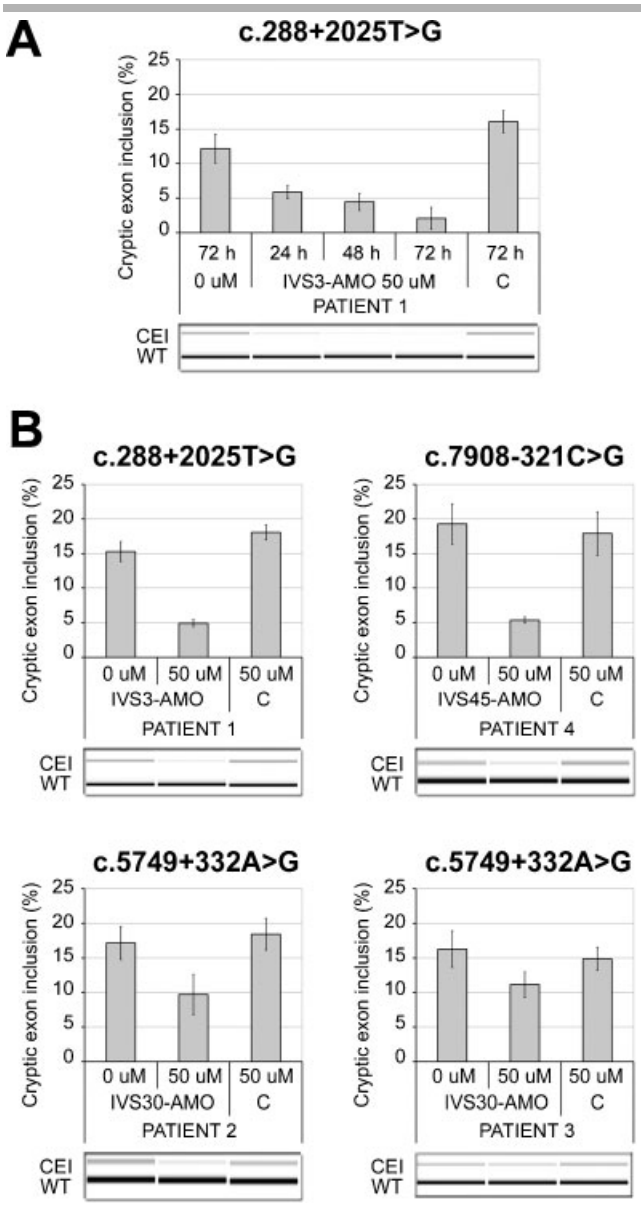


**Figure 3.** AMO treatment in EBV-transformed lymphocytes cell lines for mutations c.288+2025T>G, c.5749+332A>G, and c.7908–321C>G. **A:** Time-course results for mutation c.288+2025T>G using 50 μM AMO concentration. **B:** EBV-immortalized lymphocytes treated at 72 hr with 50 μM AMO concentration for mutations c.288+2025T>G (Patient 1), c.5749+332A>G (Patients 2 and 3), and c.7908–321C>G (Patient 4). Controls for AMO specificity (C) were: IVS30-AMO, IVS45-AMO, and IVS3-AMO for c.288+2025T>G, c.5749+332A>G, and c.7908–321C>G mutations, respectively. CEI: cryptic exon inclusion; WT: wild-type.

treatment. Wild-type transcript levels were normalized to a constitutional expressed gene (cyclophillin) (Fig. 5B). When cells were treated with the specific AMO an increase in wild-type transcripts (with respect to the level of cyclophilin) was observed, which confirms that AMO induced correct splicing by blocking the recognition of the new splice site created by the mutation.

Finally, we determined whether AMO acted specifically on the mutated *NF1* allele by analyzing the presence of polymorphic markers in the *NF1* coding region of the patients studied. We found one patient (Patient 3, c.5749+332A>G) to be polymorphic for a single nucleotide change in exon 13. We performed

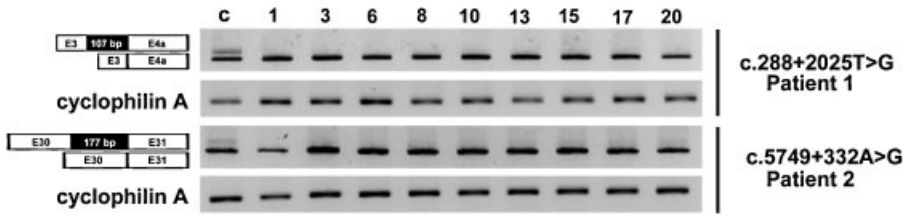


**Figure 4.** Duration of AMO treatment effect. To test the duration of the AMO effect on aberrant splicing correction, fibroblast cell lines derived from two independent patients were treated with mutation-specific AMOs and RT-PCR analysis was performed for up to 20 days (5 μM IVS3-AMO for c.288+2025T>G mutation and 30 μM IVS30-AMO for c.5749+332A>G mutation). C: control, untreated fibroblast cells.

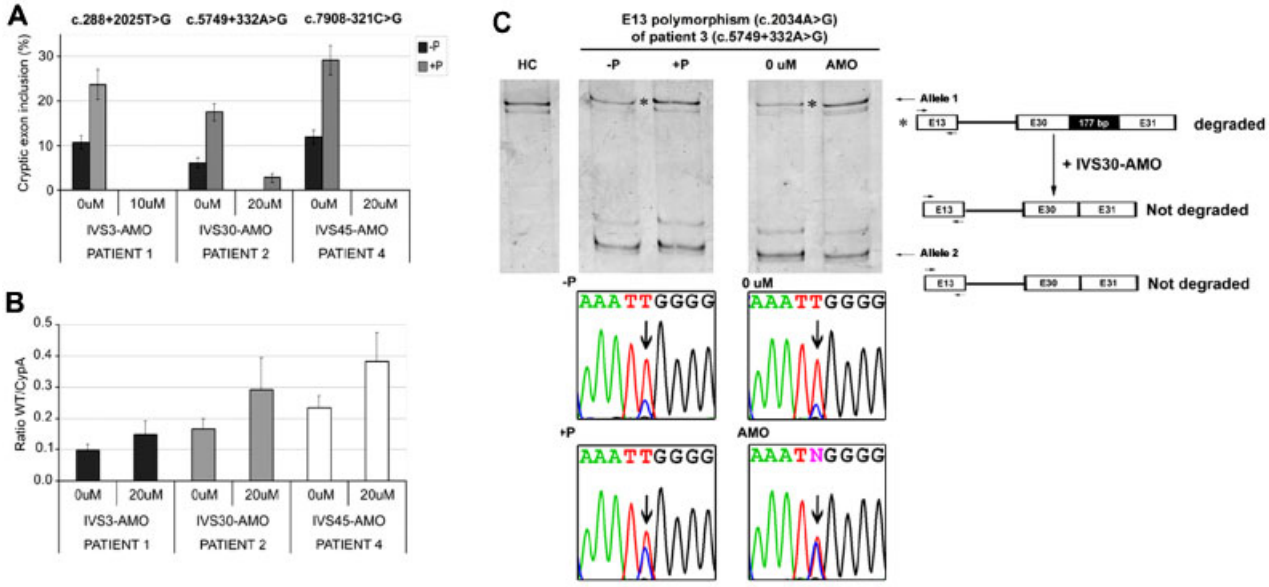


**Figure 5.** Assessing the mode of action and specificity of AMO in patients' fibroblasts. **A:** Treatment with puromycin showed that transcripts containing the cryptic exon are degraded by NMD (0 μM of AMO). Treatment with specific AMO corrected abnormal splicing even when NMD was inhibited. **B:** Wild-type *NF1* transcript normalization with cyclophilin gene expression. For all mutations studied, the proportion of WT transcript increased relative to cyclophilin transcripts after AMO treatment. **C:** Assessing the expression of both *NF1* alleles. Analysis of Exon 13 polymorphism in Patient 3 by cDNA-SSCP (upper panel) and by sequence analysis (bottom panels; reverse sequence is shown). Degradation of the upper band of cDNA-SSCP (denoted by an asterisk) and G-allele was observed in the electropherogram sequence when NMD was not prevented (−P), which suggests that Allele 1 carries both the germline mutation of Patient 3 in exon 30 (c.5749+332A>G) and the G nucleotide of the Exon 13 polymorphism (denoted by an arrow). Expression of the two alleles became equal upon treatment with puromycin (+P). When puromycin was not added, AMO treatment promoted normal splicing of the mutated allele, whose expressed mRNAs were no longer degraded by the NMD machinery. [Color figure can be viewed in the online issue, which is available at www.interscience.wiley.com.] HC: homozygous control; −P: without puromycin; +P: with puromycin; AMO: IVS30-AMO treatment.

an SSCP analysis of exon 13 region using cDNA from cultured fibroblasts, to differentiate both *NF1* alleles, and determined which allele was being degraded by the NMD mechanism, which was assumed to be the mutated allele. We then analyzed cDNA from fibroblasts treated with or without AMO. SSCP-cDNA analysis of exon 13 showed that AMO treatment recovered transcript levels of the putative mutated allele (Fig. 5C, upper panel). These results were also confirmed by sequence analysis of the polymorphism (Fig. 5C, bottom panel).

### Assessing the Effect of AMO on Neurofibromin Function

Finally, it was important to confirm that correction of aberrant splicing by AMO treatment was also observed at the functional level. Since neurofibromin function cannot be assessed directly, we conducted an indirect analysis by measuring Ras-GTP levels in fibroblast cultures, as neurofibromin is known to be a negative regulator of Ras. We treated fibroblast cultures carrying three different deep intronic mutations with or without AMO and analyzed the results against the wild-type control. Cell lysates were prepared and a Ras activation assay was performed (see Materials and Methods for details) (Fig. 6). Levels of active Ras-GTP in untreated cultures from the three patients were higher than that found in the wild-type control (Fig. 6), which is consistent with lower neurofibromin activity in mutant fibroblasts. However, Ras-GTP levels were much lower in fibroblasts treated with specific AMOs than in untreated fibroblasts, reaching levels comparable to those of wild-type control fibroblasts. This decrease in Ras-GTP levels suggests that not only did AMO treatment correct the aberrant splicing but that the correction led to the restoration of the neurofibromin GTPase activity.

## Discussion

In this study we tested the suitability of using AMOs to correct the aberrant splicing caused by deep intronic mutations in the *NF1* gene. We isolated fibroblast and lymphocyte cell lines from

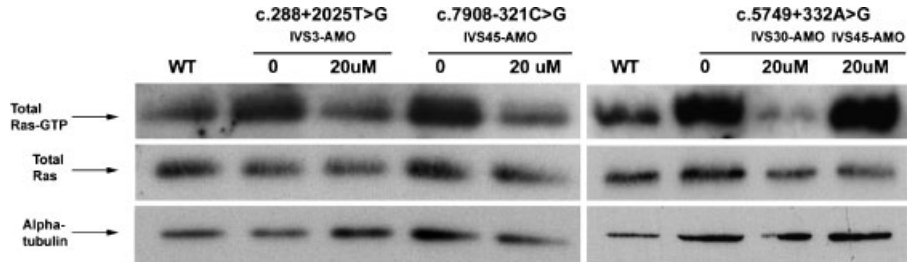


**Figure 6.** Reduction of Ras-GTP levels after AMO treatment of patients' fibroblasts. Neurofibromin GTPase activity was indirectly assessed by quantifying Ras-GTP levels in cell lysates. In all cases mutation-specific AMO treatment decreased the levels of active Ras to levels comparable to those of WT control fibroblasts, presumably by restoration of neurofibromin function. The use of a nonspecific AMO for mutation c.5749+332A>G (IVS45-AMO 20 μM) shows not effect on the levels of Ras-GTP (last column, right panel).

six NF1 patients harboring three different deep intronic *NF1* mutations. Treatment of these cell lines with specifically designed AMOs showed that this antisense approach corrected aberrant splicing and significantly increased the levels of wild-type *NF1* transcripts. We also found that AMO treatment decreased the active Ras-GTP levels in the same cells, which is consistent with the hypothetical restoration of neurofibromin GTPase activity to wild-type levels.

The effect of aberrant splicing correction by morpholinos was observed to be rapid (on the order of hours) and lasted for several days. Similar results have been obtained for propionic and methylmalonic acidemia [Rincon et al., 2007]. However, the efficiency of aberrant *NF1* splicing correction varied between mutations and the treatment had different effects depending on the cell type. Our experiments showed that different AMO concentrations and exposure times were required to create the optimal conditions for each mutation and cell type.

Several reasons could explain the differences in AMO activity between the three studied mutations, for example, differences in the strength of the cryptic acceptor/donor splice sites or variations in the extent to which AMO accesses the pre-mRNA secondary structures. Different strategies could be used to improve normal splicing for the mutation with lowest correction rate (c.5749+332A>G), which include designing a new 5′ss morpholino, using a morpholino at the 3′ss, using both 5′ss and 3′ss morpholinos together, or designing morpholinos to target exon splicing enhancer (ESE) elements. It has been reported that the use of AMOs can, in some cases, be more efficient for one of the cryptic splice sites than the other [Du et al., 2007]. In addition, a study of deep intronic mutations in intron 31 in *NF1*, using minigene constructs, showed that both cryptic splice sites are important in ensuring effective cryptic exon inclusion [Raponi et al., 2006]. If this were the case, the most effective strategy might be to block both cryptic sites using two morpholinos. In recent studies, AON approaches for the Duchenne muscular dystrophy gene were found to work correctly when they were designed to block either the corresponding ESE or the 5′ splice donor site [Gurvich et al., 2008].

We observed differences in the splicing correction achieved by morpholino treatment between fibroblast and lymphocyte cell lines derived from the same patient. In all cases the lymphocytes required a higher concentration of morpholino and a longer treatment time for an equal effect to be observed. We believe that the differences between the effects observed in fibroblasts and lymphocytes could be explained by the inherent difficulty of transfecting lymphocyte cell lines [Galletti et al., 2007; Seiffert et al., 2007]. In a recent study using electroporation to deliver morpholino into cells, the authors achieved similar transfection efficiency in dermal fibroblasts and B-lymphocyte cell lines. However, different electroporation protocols were required for the two cell types. The authors showed that more electroporation cycles and a higher morpholino concentration were needed in lymphocytes for the same effectiveness to be achieved as in fibroblasts [Scaffidi and Misteli, 2005]. The different conditions required for the two cell types used in the present study are consistent with findings presented by other groups using the same delivery systems in lymphocytes [Du et al., 2007] and fibroblasts [Rincon et al., 2007].

We also found that the action of the designed *NF1* AMOs on the splicing mechanism was sequence-specific, since the use of a different AMO (designed for one of the other two mutations) had no effect on aberrant splicing correction. Since we were estimating the quantity of aberrant transcripts relative to the quantity of wild-type transcripts, we also examined the possibility that the action of the AMOs did not correct aberrant splicing but used other mechanisms such as enhancing the degradation of cryptic exon–containing transcripts. We first observed that a proportion of aberrant transcripts were actually being degraded by the NMD mechanism. After inhibiting the NMD machinery using puromycin, we demonstrated that AMOs corrected aberrant splicing even after substantial reduction of NMD. We then analyzed splicing correction by comparing the levels of wild-type *NF1* transcripts to those of a constitutionally expressed gene (in our system, cyclophilin). AMO treatment clearly increased the pool of wild-type *NF1* transcripts. Finally, we analyzed a heterozygous SNP in exon 13 and found that the *NF1* allele degraded by the NMD mechanism (putatively the *NF1* mutated allele) was the same one that was recovered when the specific AMO was used, in the absence of puromycin. Take together, these results suggest that AMO acts in a sequence-specific manner by preventing the splicing machinery from recognizing the newly created 5′ aberrant splice sites.

A key consideration in determining the suitability of AMOs as therapeutic tools for certain types of *NF1* mutations is whether treatment with AMO recovers neurofibromin function as well as restoring normal splicing. Since there is no direct way of assessing neurofibromin function, we measured total Ras-GTP levels to provide an indirect indication of the GTPase activity of neurofibromin. *NF1* mutated fibroblasts treated with AMOs recovered Ras-GTP levels that were similar to those of wild-type fibroblasts, which is consistent with the putative restoration of normal neurofibromin GTPase activity. This result has a significant bearing on the potential therapeutic application of AMOs. Consequently, our results are in agreement with those of recent studies in which AMOs were used in the treatment of other genetic disorders [Aartsma-Rus et al., 2003, 2004; Du et al., 2007; Mann et al., 2001; McClorey et al., 2006; Rincon et al., 2007; Suwanmanee et al., 2002b]. Notably, intramuscular administration of these therapeutic tools to human patients has yielded promising

results for Duchenne muscular dystrophy patients [van Deutekom et al., 2007].

In conclusion, our results suggest that AMOs could be used as a therapeutic tool for patients suffering from this autosomal dominant genetic disease bearing *NF1* deep intronic mutations. In addition, the same or similar therapeutic strategies could possibly be applied to other types of *NF1* mutations as well as to other genetic disorders. As such, it would be interesting to examine the effects of similar antisense agents on these types of mutations and to initiate in vivo assays with animal models.

## Acknowledgments

We thank all patients and relatives who participated in this study. Conxi Lázaro wishes to offer special thanks to Belén Pérez and Lourdes R. Desviat for inspiring the present study at the EMBO Conference "Pre-mRNA Processing and Disease," held in Cortina d'Ampezzo (Italy) in January 2007.

## References

Aartsma-Rus A, Janson AA, Kaman WE, Bremmer-Bout M, den Dunnen JT, Baas F, van Ommen GJ, van Deutekom JC. 2003. Therapeutic antisense-induced exon skipping in cultured muscle cells from six different DMD patients. Hum Mol Genet 12:907–914.

Aartsma-Rus A, Janson AA, Kaman WE, Bremmer-Bout M, van Ommen GJ, den Dunnen JT, van Deutekom JC. 2004. Antisense-induced multiexon skipping for Duchenne muscular dystrophy makes more sense. Am J Hum Genet 74:83–92.

Andreutti-Zaugg C, Scott RJ, Iggo R. 1997. Inhibition of nonsense-mediated messenger RNA decay in clinical samples facilitates detection of human MSH2 mutations with an in vivo fusion protein assay and conventional techniques. Cancer Res 57:3288–3293.

Ars E, Serra E, Garcia J, Kruyer H, Gaona A, Lazaro C, Estivill X. 2000. Mutations affecting mRNA splicing are the most common molecular defects in patients with neurofibromatosis type 1 [Erratum: Hum Mol Genet 2000;9:659]. Hum Mol Genet 9:237–247.

Burge C. 1998. Modeling dependencies in pre-mRNA splicing signals. Computational methods in molecular biology. Philadelphia: Elsevier Science. p 129–164.

De Raedt TM, Maertens O, Serra E, Legius E. 2008. Somatic *NF1* mutations in tumors and other tissues. In: Kaufmann D, editor. Neurofibromatoses. Monogr Hum Genet. Basel, Karger, vol 16, p 143–153.

Du L, Pollard JM, Gatti RA. 2007. Correction of prototypic ATM splicing mutations and aberrant ATM function with antisense morpholino oligonucleotides. Proc Natl Acad Sci USA 104:6007–6012.

Friedman KJ, Kole J, Cohn JA, Knowles MR, Silverman LM, Kole R. 1999. Correction of aberrant splicing of the cystic fibrosis transmembrane conductance regulator (CFTR) gene by antisense oligonucleotides. J Biol Chem 274:36193–36199.

Galletti R, Masciarelli S, Conti C, Matusali G, Di Renzo L, Meschini S, Arancia G, Mancini C, Mattia E. 2007. Inhibition of Epstein Barr Virus LMP1 gene expression in B lymphocytes by antisense oligonucleotides: uptake and efficacy of lipid-based and receptor-mediated delivery systems. Antiviral Res 74:102–110.

Gurvich OL, Tuohy TM, Howard MT, Finkel RS, Medne L, Anderson CB, Weiss RB, Wilton SD, Flanigan KM. 2008. DMD pseudoexon mutations: splicing efficiency, phenotype, and potential therapy. Ann Neurol 63:81–89.

Lacerra G, Sierakowska H, Carestia C, Fucharoen S, Summerton J, Weller D, Kole R. 2000. Restoration of hemoglobin A synthesis in erythroid cells from peripheral blood of thalassemic patients. Proc Natl Acad Sci USA 97:9591–9596.

Li Y, O'Connell P, Breidenbach HH, Cawthon R, Stevens J, Xu G, Neil S, Robertson M, White R, Viskochil D. 1995. Genomic organization of the neurofibromatosis 1 gene (NF1). Genomics 25:9–18.

Mann CJ, Honeyman K, Cheng AJ, Ly T, Lloyd F, Fletcher S, Morgan JE, Partridge TA, Wilton SD. 2001. Antisense-induced exon skipping and synthesis of dystrophin in the mdx mouse. Proc Natl Acad Sci USA 98:42–47.

McClorey G, Fall AM, Moulton HM, Iversen PL, Rasko JE, Ryan M, Fletcher S, Wilton SD. 2006. Induced dystrophin exon skipping in human muscle explants. Neuromuscul Disord 16:583–590.

Messiaen L, Wimmer K. 2008. *NF1* mutational spectrum. In: Kaufmann D, editor. Neurofibromatoses. Monogr Hum Genet. Basel, Karger, vol 16, p 63–77.

Pluvinet R, Petriz J, Torras J, Herrero-Fresneda I, Cruzado JM, Grinyo JM, Aran JM. 2004. RNAi-mediated silencing of CD40 prevents leukocyte adhesion on CD154-activated endothelial cells. Blood 104:3642–3646.

Pros E, Gomez C, Martin T, Fabregas P, Serra E, Lazaro C. 2008. Nature and mRNA effect of 282 different NF1 point mutations: focus on splicing alterations. Hum Mutat 29:E173–E193.

Raponi M, Upadhyaya M, Baralle D. 2006. Functional splicing assay shows a pathogenic intronic mutation in neurofibromatosis type 1 (NF1) due to intronic sequence exonization. Hum Mutat 27:294–295.

Reese MG, Eeckman FH, Kulp D, Haussler D. 1997. Improved splice site detection in Genie. J Comput Biol 4:311–323.

Regnier V, Danglot G, Nguyen VC, Bernheim A. 1995. A Tsp509I variant in exon 13 of the neurofibromatosis type 1 (NF1) gene allows the identification of both alleles at the mRNA level [Erratum: Hum Genet 1995;96:744]. Hum Genet 96:131–132.

Riccardi VM. 1992. Neurofibromatosis: phenotype, natural history and pathogenesis. Baltimore: Johns Hopkins University Press. 498pp.

Rincon A, Ugarte M, Aguado C, Desviat LR, Sanchez-Alcudia R, Perez B. 2007. Propionic and methylmalonic acidemia: antisense therapeutics for intronic variations causing aberrantly spliced messenger RNA. Am J Hum Genet 81:1262–1270.

Scaffidi P, Misteli T. 2005. Reversal of the cellular phenotype in the premature aging disease Hutchinson-Gilford progeria syndrome. Nat Med 11:440–445.

Seiffert M, Stilgenbauer S, Dohner H, Lichter P. 2007. Efficient nucleofection of primary human B cells and B-CLL cells induces apoptosis, which depends on the microenvironment and on the structure of transfected nucleic acids. Leukemia 21:1977–1983.

Senapathy P, Shapiro MB, Harris NL. 1990. Splice junctions, branch point sites, and exons: sequence statistics, identification, and applications to genome project. Methods Enzymol 183:252–278.

Serra E, Rosenbaum T, Winner U, Aledo R, Ars E, Estivill X, Lenard HG, Lazaro C. 2000. Schwann cells harbor the somatic NF1 mutation in neurofibromas: evidence of two different Schwann cell subpopulations. Hum Mol Genet 9:3055–3064.

Serra E, Rosenbaum T, Nadal M, Winner U, Ars E, Estivill X, Lazaro C. 2001. Mitotic recombination effects homozygosity for NF1 germline mutations in neurofibromas. Nat Genet 28:294–296.

Shapiro MB, Senapathy P. 1987. RNA splice junctions of different classes of eukaryotes: sequence statistics and functional implications in gene expression. Nucleic Acids Res 15:7155–7174.

Sierakowska H, Sambade MJ, Agrawal S, Kole R. 1996. Repair of thalassemic human beta-globin mRNA in mammalian cells by antisense oligonucleotides. Proc Natl Acad Sci USA 93:12840–12844.

Summerton J, Weller D. 1997. Morpholino antisense oligomers: design, preparation, and properties. Antisense Nucleic Acid Drug Dev 7:187–195.

Suwanmanee T, Sierakowska H, Fucharoen S, Kole R. 2002a. Repair of a splicing defect in erythroid cells from patients with beta-thalassemia/HbE disorder. Mol Ther 6:718–726.

Suwanmanee T, Sierakowska H, Lacerra G, Svasti S, Kirby S, Walsh CE, Fucharoen S, Kole R. 2002b. Restoration of human beta-globin gene expression in murine and human IVS2-654 thalassemic erythroid cells by free uptake of antisense oligonucleotides. Mol Pharmacol 62:545–553.

van Deutekom JC, Bremmer-Bout M, Janson AA, Ginjaar IB, Baas F, den Dunnen JT, van Ommen GJ. 2001. Antisense-induced exon skipping restores dystrophin expression in DMD patient derived muscle cells. Hum Mol Genet 10:1547–1554.

van Deutekom JC, Janson AA, Ginjaar IB, Frankhuizen WS, Aartsma-Rus A, Bremmer-Bout M, den Dunnen JT, Koop K, van der Kooi AJ, Goemans NM, de Kimpe SJ, Ekhart PF, Venneker EH, Platenburg GJ, Verschuuren JJ, van Ommen GJ. 2007. Local dystrophin restoration with antisense oligonucleotide PRO051. N Engl J Med 357:2677–2686.

Viskochil D. 1998. Gene structure and expression. In: Upadhyaya M, Cooper DN, editors. Neurofibromatosis type1: from genotype to phenotype. Oxford: BIOS Scientific Publishers. p 39–56.

Wimmer K, Roca X, Beiglbock H, Callens T, Etzler J, Rao AR, Krainer AR, Fonatsch C, Messiaen L. 2007. Extensive in silico analysis of NF1 splicing defects uncovers determinants for splicing outcome upon 5′ splice-site disruption. Hum Mutat 28:599–612.

Xu G, Lin B, Tanaka K, Dunn D, Wood D, Gesteland R, White R, Weiss R, Tamanoi F. 1990. The catalytic domain of the neurofibromatosis type 1 gene product stimulates ras GTPase and complements IRA mutants of S. cerevisiae. Cell 63:835–841.

Yeo G, Burge CB. 2004. Maximum entropy modeling of short sequence motifs with applications to RNA splicing signals. J Comput Biol 11:377–394.